euspen's 22nd International Conference & Exhibition, Geneva, CH, May/June 2022
www.euspen.eu

Structured laser beam for alignment and large-scale metrology

Krystof Polak[1,3], Jean-Christophe Gayde[1], Miroslav Sulc[2,3]

[1]CERN – European Organization for Nuclear Research, Switzerland
[2]IPP – Institute of Plasma Physics of the Czech Academy of Sciences, Czech Republic
[3]TUL – Technical University of Liberec, Czech Republic

krystof.polak@cern.ch

Abstract

The structured laser beam (SLB) is a pseudo-non-diffractive optical beam. Its optical intensity profile in the transverse plane is similar to that of a Bessel beam. Thus, the SLB has a narrow central spot of high intensity surrounded by concentric circles. It is possible to generate a SLB such that the visibility – as defined in optics – of its central spot or concentric circles is equal to one. An interesting feature of the SLB is its ability to propagate over very long distances. It is theoretically possible to generate a SLB with an "infinite" range. The maximum distance at which SLB propagation has been tested is 200 m. Even at a distance of several hundred metres, the SLB retains its low divergence capability. During the measurement, under certain conditions, a divergence angle of less than 0.01 mrad was measured, the diameter of the central spot at the beginning of the beam being about 0.01 mm. This article summarises part of the research related to the properties of the SLB and measurements of some of its characteristics at different distances up to more than 100 m. Extensive simulations have allowed the study of phenomena such as the effect of symmetry breaking on the beam propagation, as well as the minimum dimensions of the free space required around the SLB. The capabilities of the SLB could make it attractive for the potential development of applications in alignment or large-scale metrology.

Alignment, Laser, Positioning.

1. Introduction

The Bessel beam (BB) is a type of non-diffractive optical beam. Such laser beams have been used for alignment purposes [1-3], but the fact that their length does not exceed 20 m under standard conditions is a limiting factor for their use in long-range metrology.

However, a new way of generating long-distance Structured Laser Beams (SLB) [4], with a transverse intensity profile partly similar to quasi-Bessel beams, allows to overpass this limit. SLB has special properties - some of which have been tested in the range of a few centimetres to a distance of 200 m - that appear to be of interest in the context of the development of large-scale metrology tools and high precision long range alignment systems, such as for particle accelerators. Similarly to the BB, the SLB shows, a transverse profile made of a narrow central spot of high intensity surrounded by concentric circles. In addition this type of beam has the ability to propagate up to very long distances – theoretically up to infinity - with a low divergence of the central part. It can be expected that under ideal conditions, i.e. propagation in vacuum and symmetrical distribution of the complex amplitude, a SLB will propagate strictly in a straight line.

The transverse and longitudinal profile structures as well as the divergence of the central beam are shortly described below. Then, the influence of a symmetry breaking on the propagation of the beam and on its straightness is discussed. The paper examines two types of symmetry breaking that can occur. The first one is due to the transit of the beam through a circular aperture, which is transversely shifted. The second one is obtained by blocking part of the beam on one side.

The research was conducted using numerical simulations. In this study, the propagation of the beam is considered under vacuum in order to avoid the influence of the gradient distribution of the refractive index of the atmosphere.

The resulting data should provide an indicative knowledge of the shift of the SLB centre for the given conditions. This knowledge will then be used in future work to set the parameters of the experiments for verification of the simulations.

2. SLB propagation at long distances

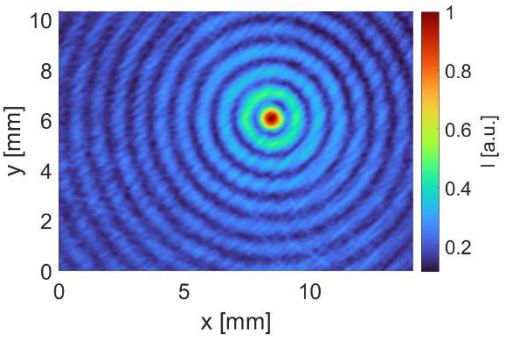

Figure 1. Image of a real SLB at a distance of 140 m from the generator. The optical intensity I is represented in arbitrary units.

2.1. The transversal profile

The traversal profile consists of a narrow central part with the highest intensity and of a surrounding part made of concentric circles, see an image of real SLB in **Figure 1Error! Reference source not found.**. Concentric light circles are separated by dark ones. As it is the case for Bessel beams, a zero optical intensity in the dark circles of a SLB is theoretically achievable.

2.2. Longitudinal profile and divergence of the core

Unlike a Bessel beam, a SLB can theoretically propagate up to infinity. The range was tested from some centimetres up to a distance of 200 m. The longitudinal profile of a SLB, see the example in **Figure 2Error! Reference source not found.**, has also other characteristics compared to a Bessel beam one.

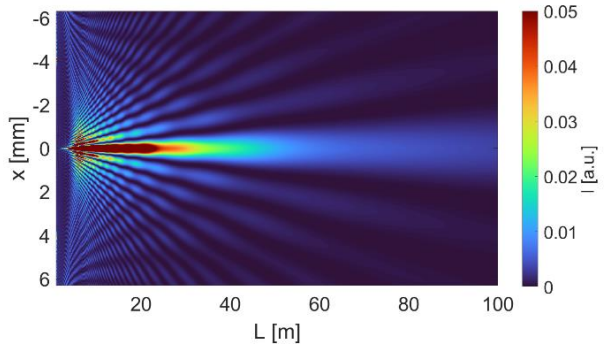

Figure 2. Computer simulation of the SLB longitudinal profile. The optical intensity I is represented in arbitrary units.

Naturally, a SLB propagating over long distances is subject to divergence. However, the cone angle at which its core diverges can be very small. The picture of a real SLB, see **Figure 1**, taken at 140 m from the generator shows a diameter of the central core of 1.3 mm. Knowing that this SLB was starting at 5 m after the generator with a diameter close to a few microns, the divergence of its central part is approximately 9.6 μrad.

3. The simulations of SLB and beam symmetry breaking

This chapter introduces the procedure and principle of the performed computer simulations describing the spread of SLBs, partially obscured by an obstacle. It explains the use of two types of obstacles that asymmetrically block parts of the SLB and presents a method for finding a SLB central spot position.

3.1. Simulation of the field just after the SLB generator

The field immediately behind the SLB generator was calculated using ray optics from the known initial illumination field (a Gaussian beam was considered). The postulates of ray optics were taken into account, and the change in the direction of the rays therefore occurred only at the interface of two media with different refractive indices based on Snell's law in a vector form [5]

$$(\overrightarrow{k_2} - \overrightarrow{k_1}) \times \vec{v} = 0. \tag{1}$$

Equation (1) expresses the fact that the tangent components of the wave vectors $\overrightarrow{k_1}$ and $\overrightarrow{k_2}$ are continuous at the interface of two media with different refractive indices. The orientation of the interface at the incident point is given by its normal vector $\vec{v}$.

The phase distribution of the SLB in the transverse plane immediately after the generator was calculated based on the optical path distance of each individual ray. Note that the SLB generator can be tuned to create various SLBs with different characteristics. More information about the generation principle is given in [4].

3.2. Simulation of the SLB propagation in free space

The further development of light, after leaving the generator, is more complicated and requires taking into account the wave nature of the light. In general, the problem can be solved using the diffraction integral [5, 6]:

$$u(x,y,z) = \frac{i}{\lambda}\iint u(\tilde{x},\tilde{y},0)\frac{e^{-ikr}}{r}\cos\theta\, d\tilde{x}\, d\tilde{y}, \tag{2}$$

where $i\cos\theta/\lambda$ is the inclination factor.

When considering a paraxial (Fresnel) approximation, the following assumptions can be made:

$$\cos\theta = \frac{z}{r} \tag{3}$$

and

$$r \approx z\left(1 + \frac{1}{2}\left(\frac{x^2+y^2}{z^2}\right)\right). \tag{4}$$

The diffraction integral is then adjusted:

$$u(x,y,z) = \frac{i}{\lambda}\iint u(\tilde{x},\tilde{y},0)\, e^{-ikr} e^{-\frac{i\pi}{\lambda z}((x-\tilde{x})^2+(y-\tilde{y})^2)}\, d\tilde{x}\, d\tilde{y}, \tag{5}$$

and after further modifications, the diffraction integral will take the form:

$$u(x,y,z) = \frac{i}{\lambda z} e^{-\frac{i\pi}{\lambda z}(x^2+y^2)} \tilde{U}\left(\frac{x}{\lambda z}, \frac{y}{\lambda z}\right), \tag{6}$$

where $\tilde{U} = FT\{\tilde{u}\}$ is a Fourier transform of the modified aperture function $\tilde{u} = u(\tilde{x},\tilde{y},0)e^{-\frac{i\pi}{\lambda z}(\tilde{x}^2+\tilde{y}^2)}$.

Following the process below, the complex amplitude of the beam is calculated at any distance:

1. The SLB is traced from the generator to the obstacle using the Fresnel diffraction integral;
2. In the obstacle plane, the calculated field is multiplied by a window function representing the obstacle;
3. The Fresnel diffraction integral is used again to trace the SLB after crossing the obstacle up to the demanded position.

3.3. Two types of obstacles

The 2 types of obstacles used in the simulations are considered to be ideal ones. That means perfectly impermeable screens, through which no parasitic field seeps. In the numerical simulations, the obstacles were realized by assigning a zero value of the complex amplitude in the part of the beam blocked by the screen. The situation is illustrated in **Figure 3**, which shows the simulation of the corresponding optical intensity distribution in the plane just after the obstacle. More specifically, it is a beam passing through a circular aperture shifted with respect to the beam axis. The position of the circular aperture is defined by the coordinates of its centre $[x_{c0}, y_{c0}]$.

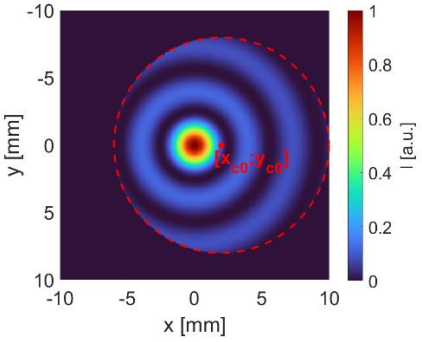

Figure 3. Computer simulation of the SLB after using an obstacle with a circular aperture. $[x_{c0}, y_{c0}]$ are the coordinates of the circular aperture centre.

The similar situation with a different type of obstacle, i.e. only part of the SLB covered on one side, is shown in **Figure 4**. The δx parameter therefore specifies the position of the obstacle edge on the x-axis. The edge of the obstacle is perpendicular to the x-axis.

3.4. SLB centre position detection

The method used to accurately evaluate the position of the simulated SLB centre, which was proved successful in measuring the position of real SLBs, is based on the similarity between SLB and Bessel beam. As part of the optimization, the parameters of the equation describing the Bessel beam are sought to find the optimal agreement with the investigated SLB. Equation (7) describes the optical intensity distribution $I(x, y)$ of a Bessel beam with the centre intensity normalized to one.

$$I(x,y) = \left(J_0\left(k_T\sqrt{(x-x_0)^2+(y-y_0)^2}\right)\right)^2, \qquad (7)$$

where J_0 is Bessel function of the first kind and zero order, k_T is the transverse wave vector and $[x_0; y_0]$ are the coordinates of the centre of the Bessel beam. The parameters k_T, x_0 and y_0 are subject to change during the optimization process. After finding the parameters for which the analytical relation best fits the observed SLB, the coordinates $[x_0; y_0]$ are used as the centre position of the SLB.

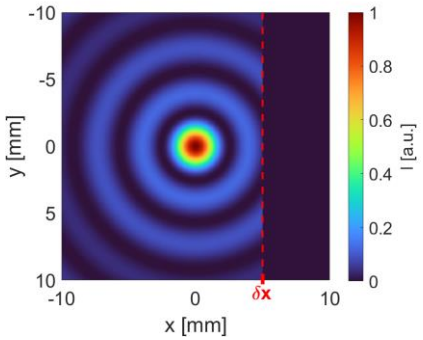

Figure 4. Computer simulation of the SLB after using an obstacle on one side of the beam. The δx parameter is the x coordinate of the obstacle edge.

3.5. Summary of assumptions and limitations

- The beam propagation medium is the vacuum.
- The polarisation is negligible for the type of SLB generator which is considered here.
- The simulations are based on wave optics.
- The solution of the diffraction integral uses Fresnel approximations. The error of this approximation decreases with distance from the source field. This means that the error for the simulations considered here is negligible.
- The obstacles are completely opaque and do not leak even parasitic fields.
- The beam centre detection method is applied only on the beam part where circles are fully visible.

4. Parameters and results of simulations

Six types of simulations were performed in total. The nature of each simulation is described by the following parameters:

- The type of the obstacle;
- The distance L_O of the obstacle from the SLB generator;
- The diameter D of the aperture if the obstacle is a circular one.

The distance L_O is either 10 m or 100 m in the performed simulations. The value of 10 m corresponds to a distance inside the near zone, the so-called Fresnel zone, in which the beam shape changes depending on the longitudinal coordinates. The value of 100 m corresponds to the far zone, the so-called Fraunhofer zone, in which the beam shape no longer changes with longitudinal coordinates and where only the size is linearly increasing.

The results of all simulations are visualized in graphs. The shift Δx of the SLB centre position is shown by the colour axis and depends on two parameters. The first one is the distance L from the obstacle and is common for all simulations. Specifically, L takes values from 20 m to 1000 m. The second one is either x_{c0} for the circular aperture, see **Figure 3**, or δx for SLB with one-side blocking, see **Figure 4**. The lower limit of the δx parameter was chosen so that obvious deformations did not appear in the vicinity of the SLB centre. The upper limit of the δx parameter was chosen bigger than the largest circle of the SLB.

For the one-side SLB blocking results, the graph was divided into 2 zones with 2 different colour scales for the Δx axis. This was done with the intention of making visible small Δx values and their changes that would not be seen on a common scale.

4.1. Results of simulations

The obtained results are visualized in **Figure 5** – **Figure 10**.

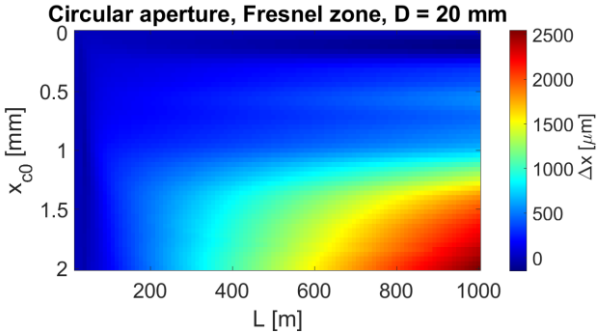

Figure 5. The Δx shift of the SLB centre depends on the distance L from the obstacle and on the position of the circular aperture described by the x_{c0} coordinate. The obstacle hole has a 20 mm diameter and is placed at 10 m from the SLB generator, i.e. in the Fresnel zone.

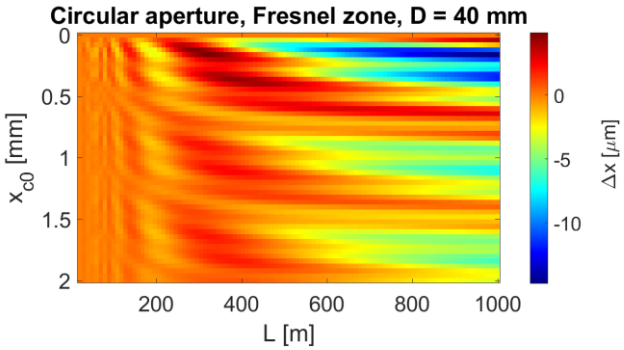

Figure 6. The Δx shift of the SLB centre depends on the distance L from the obstacle and on the position of the circular aperture described by the x_{c0} coordinate. The obstacle hole has a diameter of 40 mm and is placed at 10 m from the SLB generator, i.e. in the Fresnel zone.

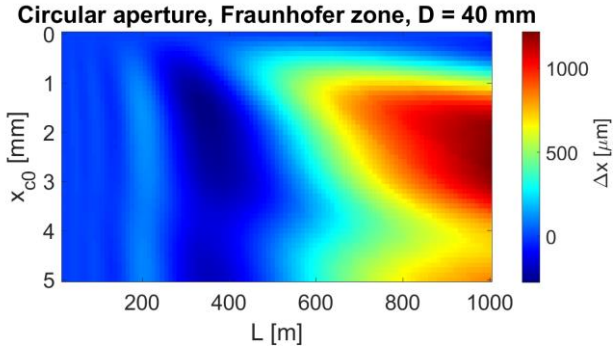

Figure 7. The Δx shift of the SLB centre depends on the distance *L* from the obstacle and on the position of the circular aperture described by the x_{c0} coordinate. The obstacle hole has a diameter of 40 mm and is placed at 100 m from the SLB generator, i.e. in the Fraunhofer zone.

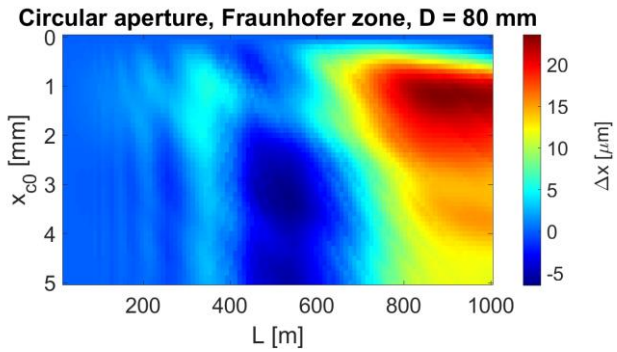

Figure 8. The Δx shift of the SLB centre depends on the distance *L* from the obstacle and on the position of the circular aperture described by the x_{c0} coordinate. The hole in the obstacle has a diameter of 80 mm and is placed at a distance of 100 m from the SLB generator, i.e. in the Fraunhofer zone.

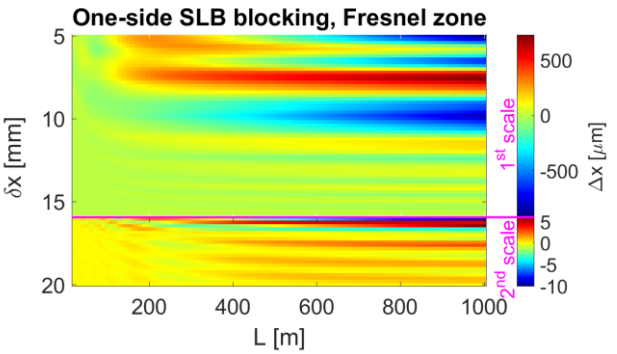

Figure 9. The Δx shift of the SLB centre depends on the distance from the obstacle and on the δx parameter. The obstacle is placed at a distance of 10 m from the SLB generator, i.e. in the Fresnel zone.

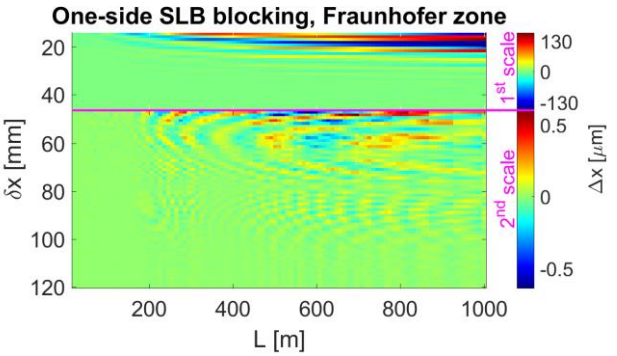

Figure 10. The Δx shift of the SLB centre depends on the distance from the obstacle and on the δx parameter. The obstacle was located at a distance of 100 m from the SLB generator, i.e. in the Fraunhofer zone.

5. Discussion of results

The results of the simulations with a circular aperture show that the diameter of the aperture has a huge effect on the SLB's centre shift Δx. For both Fresnel and Fraunhofer zones, Δx shift values up to thousands of microns were observed for small aperture diameters (*D* = 20 mm and *D* = 40 mm, respectively), see **Figure 5** and **Figure 7**. By simply doubling the diameter of the aperture, Δx was reduced to values in tens of microns range, see **Figure 6** and **Figure 8**.

An interesting phenomenon was observed mainly in the simulations with the large diameter circular apertures, see **Figure 6** and **Figure 8**. The maximum value of Δx is found for coordinates x_{c0} close to zero and, as expected, for the maximum value of *L*. For example, in **Figure 6**, the maximum Δx, approximately 15 microns, is observed for values of the parameters L and x_{c0} respectively close to 1000 m and 0.2 mm. This looks unnatural because for $x_{c0} = 0$ the SLB is symmetric and Δx is zero. A hypothesis is that this phenomenon is due to the fact that with a small shift of the centre of the circular aperture from the centre of the SLB, the aperture overlaps with one of the SLB circles over a significant portion of the circumference. The contribution of the diffraction caused by the circular aperture is consequently non-negligible in the distribution of the light intensity measured in the transverse plane studied.

In the case of an obstacle blocking one side of the SLB, see **Figure *9*** and **Figure 10**, for a same distance *L*, the Δx value oscillates around zero as the δx parameter increases. It seems interesting that the phase of oscillations does not change much with the distance. In other words, it exists δx parameter values for which the Δx value approaches zero over a long range of distances *L*. As expected, the amplitude of the oscillations decreases with increasing δx parameter. The effect of constant phases of oscillations will be closely monitored in the future.

6. Conclusion

The use of SLB as reference fiducial line for alignment over long distances looks promising.

On one hand, the long distance propagation capability and the low divergence of the central part of the beam, which keeps the central spot of small size, are major advantages.

On another hand, even if the simulations shows that a symmetry breaking of the SLB in the transverse plane leads to shift of the beam line, these shifts can be reduced at the micron level at long distances when the apertures of optical elements and the free space surrounding the beam axis are reasonably large. Note also that the simulations have been performed for one SLB longitudinal profile type, which can be easily tuned and optimised. This numerical study has to be confirmed by experiments in the near future.

In the frame of developments of alignment systems based on SLB, this work will help to define the necessary aperture around the beam according to the longitudinal range of the system and to the requested precision.

References

[1] D. M. Gale, "Visual alignment of mechanical structures using a Bessel beam - datum practical implementation", in Optical Measurement Systems for Industrial Inspection Vii, Bellingham, 2011, 8082, 80823D.

[2] R. E. Parks, "Aligning reflecting optics with Bessel beams", in Proc. SPIE 11488, Optical System Alignment, Tolerancing, and Verification XIII, Online Only, United States, 2020, 114880J.

[3] R. E. Parks, "Practical considerations for using grating produced Bessel beams for alignment purposes", in Optomechanics and Optical Alignment, Bellingham, 2021, 11816, 1181603.

[4] Sulc, M., & Gayde, J.-C. (2019), "An Optical System for Producing a Structured Beam", European patent application 3564734 A1. 2019-11-06.

[5] Born, Max; Wolf, Emil (1999), "Principles of optics: electromagnetic theory of propagation, interference and diffraction of light (7th ed.)", London; New York; Paris: Pergamon Press.

[6] Saleh, B. E. A., & Teich, M. C. (2019). "Fundamentals of Photonics: 2 Volume Set (3rd ed.)", Wiley-Blackwell. Volume **1.**